Bacterial marginolactones trigger formation of algal gloeocapsoids, protective aggregates on the verge of multicellularity

Mario K. C. Krespach[a,b], Maria C. Stroe[a], Michal Flak[a,b], Anna J. Komor[b,c], Sandor Nietzsche[d], Severin Sasso[e], Christian Hertweck[b,c], and Axel A. Brakhage[a,b,1]

[a]Department of Molecular and Applied Microbiology, Leibniz Institute for Natural Product Research and Infection Biology, Jena 07745, Germany; [b]Institute of Microbiology, Friedrich Schiller University Jena, Jena 07745, Germany; [c]Department of Biomolecular Chemistry, Leibniz Institute for Natural Product Research and Infection Biology, Jena 07745, Germany; [d]Electron Microscopy Center, University Hospital Jena 07743 Jena, Germany; and [e]Department of Plant Physiology, Institute of Biology, Leipzig University, Leipzig 04103, Germany

Edited by Jens Nielsen, BioInnovation Institute, DK2200 Copenhagen, Denmark, and approved September 30, 2021 (received for review January 15, 2021)

Photosynthetic microorganisms including the green alga *Chlamydomonas reinhardtii* are essential to terrestrial habitats as they start the carbon cycle by conversion of CO_2 to energy-rich organic carbohydrates. Terrestrial habitats are densely populated, and hence, microbial interactions mediated by natural products are inevitable. We previously discovered such an interaction between *Streptomyces iranensis* releasing the marginolactone azalomycin F in the presence of *C. reinhardtii*. Whether the alga senses and reacts to azalomycin F remained unknown. Here, we report that sublethal concentrations of azalomycin F trigger the formation of a protective multicellular structure by *C. reinhardtii*, which we named gloeocapsoid. Gloeocapsoids contain several cells which share multiple cell membranes and cell walls and are surrounded by a spacious matrix consisting of acidic polysaccharides. After azalomycin F removal, gloeocapsoid aggregates readily disassemble, and single cells are released. The presence of marginolactone biosynthesis gene clusters in numerous streptomycetes, their ubiquity in soil, and our observation that other marginolactones such as desertomycin A and monazomycin also trigger the formation of gloeocapsoids suggests a cross-kingdom competition with ecological relevance. Furthermore, gloeocapsoids allow for the survival of *C. reinhardtii* at alkaline pH and otherwise lethal concentrations of azalomycin F. Their structure and polysaccharide matrix may be ancestral to the complex mucilage formed by multicellular members of the *Chlamydomonadales* such as *Eudorina* and *Volvox*. Our finding suggests that multicellularity may have evolved to endure the presence of harmful competing bacteria. Additionally, it underlines the importance of natural products as microbial cues, which initiate interesting ecological scenarios of attack and counter defense.

microbial interaction | multicellularity | evolution | natural products | morphology

Soil is an extremely densely populated habitat, and hence, microbial interactions are nearly inevitable (1). Green algae are often overlooked when soil ecosystems are discussed despite their pivotal role as primary producers of organic carbohydrates fixing roughly 39 g carbon per square meter of soil per year (2, 3). As photosynthetic microorganisms, algae convert CO_2 to energy-rich organic carbon sources and thereby refuel the carbon cycle. The green alga *Chlamydomonas reinhardtii* is a common member of wet soils and is hence subject to biotic and abiotic stress (2, 4, 5). Stress leads to the development of adaptive mechanisms that enable survival and increase the evolutionary fitness of microorganisms. *Chlamydomonas* spp. react to NaCl stress (6), Ca^{2+} deprivation, ethylenediaminetetraacetic acid (EDTA), organic acids (7, 8), chloroplatinic acid (9), phosphate limitation (10), acidic pH (11), and sublethal levels of pollutants (12) with the production of palmelloids, which are characterized by multiple rounds of failure of daughter cells to escape the parental cell wall after cell division. *Chlorella vulgaris* forms palmelloids when treated with ecdysteroids (13). The term palmelloid is a catch-all term that originates in reference to the genus of green algae *Palmella*, which typically grows in a cell cluster (6, 14). *Chlamydomonas* spp. can also actively produce aggregates which are phenotypically different to palmelloids and serve to defend the algae against harsh stress (14–16).

In addition to abiotic stressors, there are also biotic stressors such as competition and predation. When *C. reinhardtii* is threatened by the rotifer predator *Brachionus calyciflorus*, the green alga forms palmelloids (17). *Paramecium tetraurelia* is also a predator of *C. reinhardtii*, which likely drove the evolution of *C. reinhardtii* into multicellular aggregates in response to this constant pressure by predation (18). Palmeloid aggregates are too big in diameter to be engulfed by *P. tetraurelia* and thus are protected. Another biotic stress is exerted by natural products, low molecular mass compounds with various biological activities often produced by neighboring microorganisms (19). For instance, the bacterium *Pseudomonas protegens* produces the cyclic lipopeptide orfamide A, which leads to the deflagellation of *C. reinhardtii* (20). Other microorganisms accompanying algae in wet soils are

Significance

The physiological and ecological importance of natural products often remains obscured. Here, we report that *Streptomyces*-derived marginolactones, a distinct group of soil-borne natural products, specifically trigger the formation of gloeocapsoids, previously undescribed protective aggregate structures produced by the unicellular green alga *Chlamydomonas reinhardtii*. Gloeocapsoids are distinct palmelloids differing in their protective capability toward azalomycin F. The presence of marginolactone biosynthesis gene clusters in numerous streptomycetes, their ubiquity in soil, and our observation that three different members of this natural product group trigger the formation of gloeocapsoids suggest a cross-kingdom competition with ecological relevance. In the course of evolution, the polysaccharide matrix may have developed from a transient protective feature into the foundation of true multicellularity because of sustained marginolactone stress.

Author contributions: M.K.C.K. and A.A.B. designed research; M.K.C.K., M.C.S., M.F., A.J.K., and S.N. performed research; A.J.K., S.N., and C.H. contributed new reagents/analytic tools; M.K.C.K., M.C.S., M.F., A.J.K., S.N., S.S., C.H., and A.A.B. analyzed data; and M.K.C.K. and A.A.B. wrote the paper.

The authors declare no competing interest.

This article is a PNAS Direct Submission.

[1]To whom correspondence may be addressed. Email: axel.brakhage@leibniz-hki.de.

This article contains supporting information online at http://www.pnas.org/lookup/suppl/doi:10.1073/pnas.2100892118/-/DCSupplemental.

Published November 5, 2021.

streptomycetes, known to be prolific producers of natural products (1). These filamentous bacteria are known to readily interact with other microorganisms. A well-known example is given by *Streptomyces iranensis* that induces otherwise silent natural product biosynthesis gene clusters in the fungi *Aspergillus nidulans* and *Aspergillus fumigatus* (21, 22). The products of *A. nidulans*, orsellinic acid, and lecanoric acid represent metabolites first described in lichens (23). *A. fumigatus* reacts to the streptomycete by the production of fumigermin, which inhibits the germination of spores of several *Streptomyces* species (22). However, these interactions are not exclusive to fungi but also include algae. Recently, we demonstrated that *S. iranensis* specifically released the algicidal marginolactone azalomycin F (*SI Appendix*, Fig. 1*A*) in the presence of *C. reinhardtii*. The alga survived this attack by taking shelter in the mycelium of *A. nidulans* (24). Whether the alga senses azalomycin F and reacts to the compound remained unknown. Here, we describe the discovery of an alternative strategy for the algae to cope with toxin stress without a fungal partner: the formation of so-called gloeocapsoids, a distinct type of palmelloids differing in function and based on a close resemblance of the gloeocapsoid structure to cyanobacteria of the genera *Gloeocapsa* and *Gloeothece* (25). We propose that gloeocapsoid formation is an active protective behavior induced by membrane-targeting marginolactones like azalomycin F, desertomycin A, and monazomycin. Additionally, we propose that the formation of transient cell aggregates like gloeocapsoids could have led to the evolution of multicellular green algae such as *Eudorina* and *Volvox*.

Results

Sublethal Azalomycin F Induces the Formation of Multicellular Aggregates. *C. reinhardtii* is protected from otherwise lethal concentrations of azalomycin F when it is in contact with the filamentous fungus *A. nidulans* (24). We aimed to address the question of whether the alga can also survive without a partner microorganism. When grown on Tris-acetate-phosphate (TAP) agar, *C. reinhardtii* raised the local pH, indicated by the pH indicator dye bromothymol blue (*SI Appendix*, Fig. 2*A*) (26). This alkalization is due to an uptake of acetate from the medium. Previously, streptomycetes were shown to raise the surrounding pH by the release of volatile ammonia to inhibit neighboring bacteria (27). Alkaline pH, in turn, decreased killing of *C. reinhardtii* by *S. iranensis* as well as the activity of azalomycin F in solid medium (*SI Appendix*, Fig. 2 *B* and *C*). To evaluate reduced toxicity in liquid medium, purified azalomycin F was added to *C. reinhardtii* cultured in media with a pH range of 7 to 9. As a proxy for viability, the autofluorescence of *C. reinhardtii* chlorophyll was quantified (28). At pH 7, 5 μg · mL^{-1}, azalomycin F was sufficient to kill most *C. reinhardtii* cells (*SI Appendix*, Fig. 2*D*), an effect not observed when the alga was cultivated in medium with pH 8 or 9. When *C. reinhardtii* was grown in TAP medium at pH 8 or 9, the autofluorescence dropped after 24 h but recovered after 3 to 4 d and reached levels of the untreated controls. Recovery from azalomycin F exposure was not observed in *C. reinhardtii* grown at pH 7. Samples taken from cultures at pH 8 and 9 and treated with azalomycin F formed an algal lawn on TAP agar, demonstrating the survival of algal cells, while agar plates from cultures treated with azalomycin F at pH 7 only showed few algal colonies (*SI Appendix*, Fig. 3).

Microscopic inspection of *C. reinhardtii* treated with 5 μg · mL^{-1} azalomycin F at pH 8 after 7 d of incubation revealed that multicellular aggregates surrounded by a spacious matrix had formed (Fig. 1*A*). The staining of these aggregates with fluorescently labeled concanavalin A binding to α-mannopyranosyl and α-glucopyranosyl residues found in the cell wall and the plasma

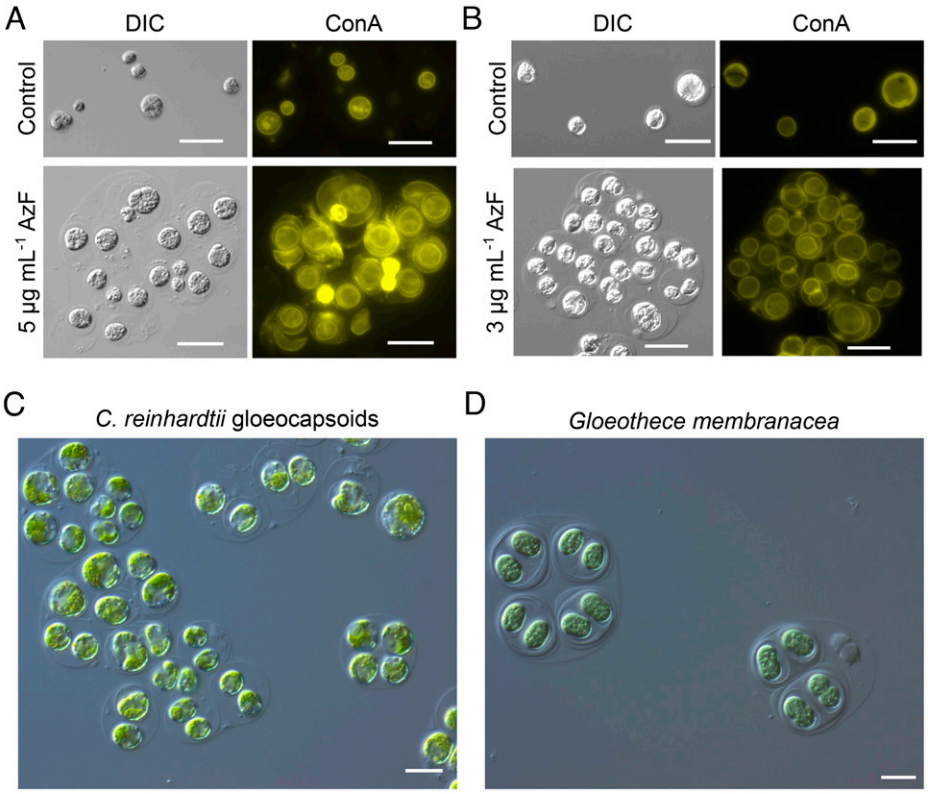

Fig. 1. *C. reinhardtii* forms gloeocapsoids in contact with sublethal concentrations of azalomycin F. (*A*) *C. reinhardtii* in TAP medium at pH 8 treated with or without 5 μg · mL^{-1} azalomycin F. (*B*) *C. reinhardtii* at pH 7 treated with or without 3 μg · mL^{-1} azalomycin F. (Scale bars: 20 μm.) (*C*) Light microscopy picture of *C. reinhardtii* gloeocapsoids. (*D*) Light microscopy picture of vegetative cells of *G. membranacea*. (Scale bars: 10 μm.)

membrane of *C. reinhardtii* illustrates the presence of multiple cell envelopes around individual cells (Fig. 1*A*). To study whether these aggregates are formed only at alkaline pH, *C. reinhardtii* was treated with 3 μg · mL^{-1} azalomycin F at pH 7. In this case, *C. reinhardtii* formed the same type of aggregate structures (Fig. 1*B*), suggesting that the activity of azalomycin F decreases at alkaline pH. The staining of the plasma membrane with CellMask indicated the presence of multiple plasma membranes in addition to cell walls surrounding the aggregates (*SI Appendix*, Fig. 4*A*). The matrix apparently consisted of acidic polysaccharides as indicated with Alcian blue staining (*SI Appendix*, Fig. 4*B*). Alcian blue stains sulfate groups of polysaccharides at pH 0.5 (in 0.5 M HCl), and at pH 2.5 (in 0.5 M acetic acid), it stains other acidic functional groups (29). Blue staining of the matrix was only observed at pH 2.5, which indicates nonsulfate acidic polysaccharides. Due to the similarity of the aggregates to the vegetative growth form of cyanobacteria of the genera *Gloeocapsa* and *Gloeothece* (25), we called these structures gloeocapsoids (Fig. 1 *C* and *D*). They differ morphologically from both palmelloids and autospores, which lack a spacious matrix and contain fewer cell membranes (14, 30). Although palmelloids can be induced by different stressors, in this study, we applied two stressors, that is, high salt and sodium citrate to induce palmelloids that served as reference. NaCl-induced palmelloids accumulated lipids (6), whereas gloeocapsoids and sodium citrate–induced palmelloids appear to contain few lipid bodies (*SI Appendix*, Fig. 5). This indicates a certain degree of heterogeneity between palmelloids. In contrast to palmelloids that are surrounded by a single outer membrane (6, 18), gloeocapsoids are surrounded by several membranes. (*SI Appendix*, Fig. 4*A*). Gloeocapsoids and palmelloids have in common that in cultures synchronized by light–dark cycles, the mother cells divide during the dark phase, and the daughter cells fail to detach from each other (*SI Appendix*, Fig. 6) (31). Hence, we suggest gloeocapsoids are a distinct form of palmelloids formed to protect *C. reinhardtii* from azalomycin F.

Gloeocapsoids Form Unusual Pseudomulticellular Structures. To further substantiate our observation that *C. reinhardtii* gloeocapsoids are surrounded by multiple cell membranes and to shed further light on their structure, transmission electron microscopy images were taken. As shown in Fig. 2*A* (orange arrows), gloeocapsoids are characterized by multiple membranes and cell walls. Interestingly, one outer membrane of a gloeocapsoid showed the characteristic indent formed by one of the flagella (Fig. 2*A*, black arrows) (32), indicating that the outer membrane is a remnant of a formerly flagellated mother cell. It is possible that after division of the mother cell, the daughter cells produced a new membrane but did not separate and instead maintained the original cell membrane. Whether azalomycin F targets the flagella or not remains to be determined. We suggest deflagellation might be due to stress or impaired cell membrane integrity. Additionally, as indicated by scanning electron microscopy, the outermost cell membrane of *C. reinhardtii* gloeocapsoids appears to be perforated in comparison to vegetative cells (Fig. 2*B*), forming a net-like structure rather than a coherent membrane. Whether azalomycin F punctures holes into the outer cell membrane or whether the mechanical force exerted by the growing daughter cells is responsible for the torn outer membrane and cell wall remains to be determined.

The gloeocapsoids of *C. reinhardtii* appear to carry fewer intracellular starch granules in proximity to the pyrenoid within the chloroplast. Untreated cells contained 26.2 ± 7.9 (n = 5) starch granules per cell with 6.2 ± 2.9 in the gloeocapsoids (n = 5, Fig. 2*A*, marked "S"). Additionally, vegetative *C. reinhardtii* cells showed multiple secretory vesicles in the cell periphery (Fig. 2*A*, blue arrows), which were completely absent in the gloeocapsoids. The absence of secretory vesicles, which are often associated with cross-species communication (33, 34), supports the idea that *C. reinhardtii* cells are isolated and thus protected against external toxin stress within gloeocapsoids. The typical gloeocapsoid features described here are summarized in a schematic model in Fig. 2*C*.

Gloeocapsoids Are Transiently Formed Structures. Evolution experiments have shown that multicellular aggregates can evolve after repeated subcultivation under selection pressure caused by a predator. These evolved multicellular aggregates remain stable for many generations in the absence of selection pressure (18). By contrast, palmelloids induced by stress conditions were found to be transient (6, 12). Therefore, we addressed the question whether gloeocapsoids would still remain stable when azalomycin F pressure was relieved. As shown in Fig. 2*D*, gloeocapsoids rapidly disassembled, and flagellated single cells were detected in cultures within 4 d of cultivation after azalomycin F was removed. This indicated that gloeocapsoids are formed transiently as long as cells are exposed to stress.

Desertomycin A and Monazomycin Are Overproduced by Streptomycetes in the Presence of *C. reinhardtii*. Marginolactones are macrolides whose biosynthesis is initiated by an arginine- or ornithine-derived starter unit (35). The marginolactones azalomycin F, desertomycin A, and monazomycin share similar chemical structures (*SI Appendix*, Fig. 1 *A–C*) and are known to disturb cell membranes (36–38). Azalomycin F is specifically released by *S. iranensis* in the presence of *C. reinhardtii* (24). Therefore, we tested whether streptomycetes encoding the biosynthetic gene clusters for desertomycin A and monazomycin respond to *C. reinhardtii*. Liquid chromatography–mass spectrometry analyses demonstrated that in the presence of *C. reinhardtii*, *Streptomyces macronensis* overproduced desertomycin A (Fig. 3 *A* and *B*). Likewise, *Streptomyces mashuensis* produced increased amounts of monazomycin in the presence of the alga (Fig. 3 *D* and *E*). As shown by matrix-assisted laser desorption/ionization imaging mass spectrometry, both compounds were found in the killing zone of *C. reinhardtii* produced by the streptomycetes (Fig. 3 *B* and *E*). This indicates that marginolactones may serve to specifically target green algae since their production is triggered by *C. reinhardtii*.

Marginolactones Trigger the Formation of Gloeocapsoids. To investigate whether desertomycin A and monazomycin induce the formation of gloeocapsoids, we added both compounds to *C. reinhardtii*. Sublethal amounts of both marginolactones triggered gloeocapsoid formation by *C. reinhardtii* (Fig. 3 *C* and *F* and *SI Appendix*, Fig. 7). This result was not surprising given their considerable structural similarity to azalomycin F. Because these compounds disturb membrane integrity, we reasoned that other membrane-active compounds might also trigger gloeocapsoid formation. This was not the case as concluded from experiments with the membrane-targeting but structurally dissimilar compounds amphotericin B and daptomycin (*SI Appendix*, Fig. 1 *D* and *E*). Amphotericin B is an antimycotic macrolide, which targets ergosterols in algae (39). Sublethal concentrations of amphotericin B did not trigger gloeocapsoid formation in *C. reinhardtii* (*SI Appendix*, Fig. 8*A*). At 2 μg · mL^{-1}, amphotericin B was lethal to *C. reinhardtii* (*SI Appendix*, Fig. 8 *B* and *C*). Daptomycin is a well-known cyclic lipopeptide antibiotic, which interferes with bacterial membrane microdomains (40). As shown by the lack of formation of a polysaccharide matrix and missing multiple cell membrane layers, daptomycin only induced the formation of aggregates in *C. reinhardtii* when applied at sublethal concentrations (*SI Appendix*, Fig. 9*A*). An application of 20 μg · mL^{-1} daptomycin was lethal for *C. reinhardtii* (*SI Appendix*, Fig. 9 *B* and *C*). We thus concluded that only marginolactones such as azalomycin F, desertomycin A, and monazomycin induced formation of gloeocapsoids since natural products with a different

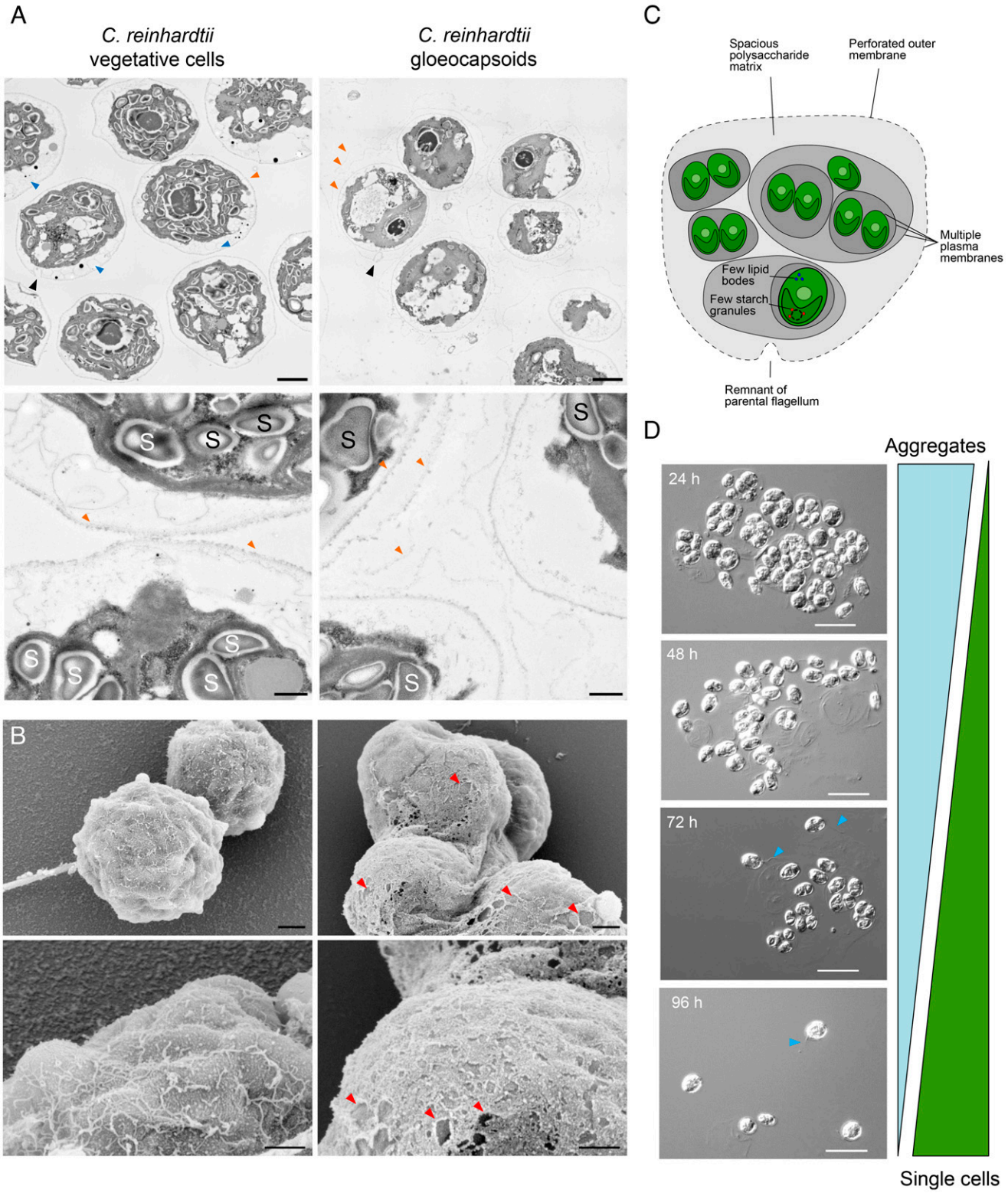

Fig. 2. Comparison of the ultrastructure of *C. reinhardtii* vegetative cells with gloeocapsoids and disassembly of gloeocapsoids after stress relief. (*A*) Transmission electron microscopy pictures of vegetative *C. reinhardtii* cells (*Left*) and gloeocapsoids (*Right*). Vegetative cells are surrounded by a single membrane (orange arrows) and contain multiple starch granules ("S"; 26.2 ± 7.9 per cell; $n = 5$). Gloeocapsoids are surrounded by up to three membranes (orange arrows) and a polysaccharide matrix. In the individual cells, there are fewer starch granules ("S"; 6.2 ± 2.9 per cell; $n = 5$). In their periphery, vegetative cells show secretory vesicles (blue arrows), which are missing in cells embedded in gloeocapsoids. (Scale bars: 2 μm [*Top*] and 500 nm [*Bottom*]). (*B*) Scanning electron microscopy pictures of *C. reinhardtii* vegetative cells (*Left*) and gloeocapsoids (*Right*). The outer membrane of vegetative cells is intact. In gloeocapsoids, the outer membrane exhibits a perforated net-like structure (holes are marked with red arrows). (Scale bars: 1 μm [*Top*] and 500 nm [*Bottom*]). (*C*) Schematic model of the structure of a gloeocapsoid. (*D*) Disassembly of gloeocapsoids after removal of azalomycin F. Flagellated single cells dominated the culture 96 h after azalomycin F was removed. Visible flagella are indicated with blue arrows. (Scale bars: 20 μm.)

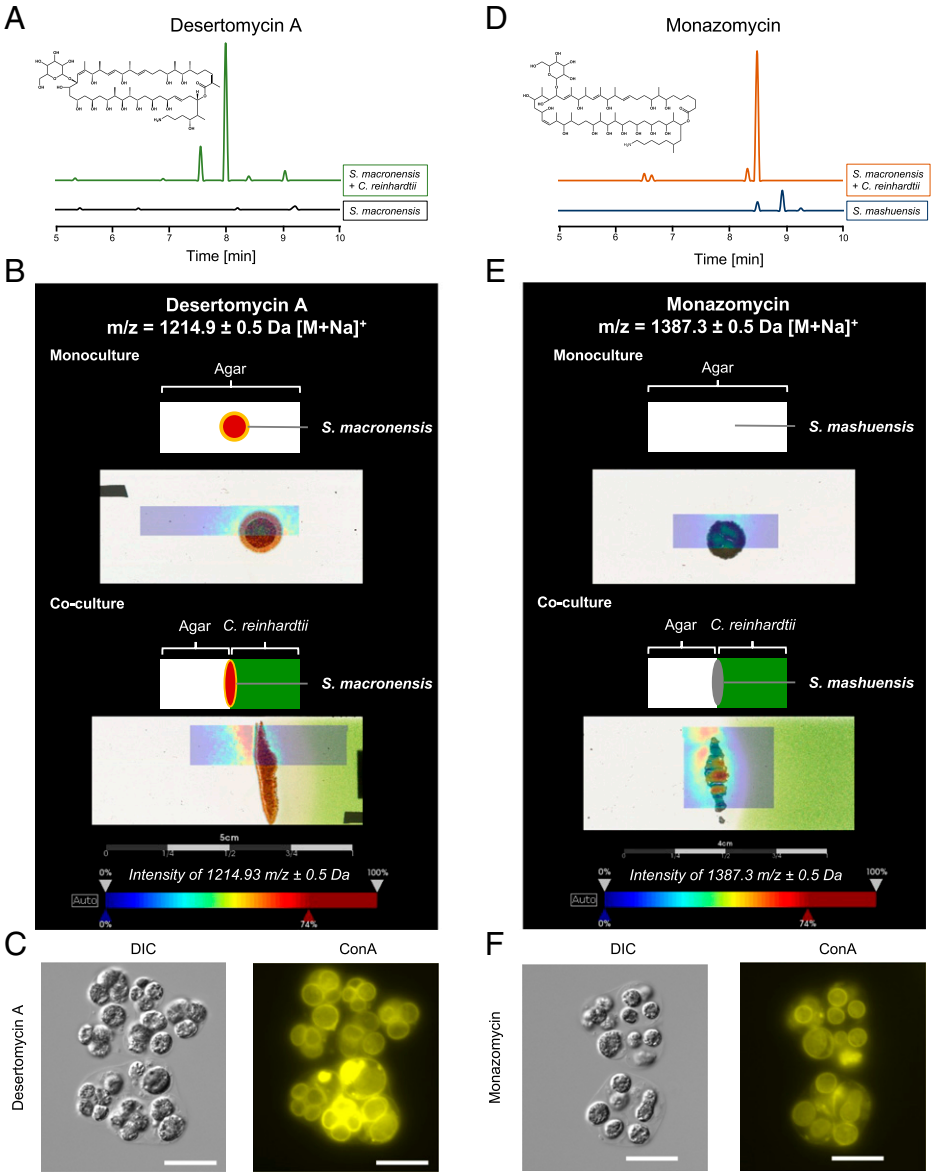

Fig. 3. Desertomycin A and monazomycin are overproduced by steptomycetes in coculture with *C. reinhardtii*, colocalize with *C. reinhardtii* killing zone on solid medium, and induce gloeocapsoid formation. (*A*) Extracted ion chromatogram of an extract of a coculture of *C. reinhardtii* with *S. macronensis* in liquid culture compared with a monoculture of the streptomycete. *m/z* 1,191.2 to 1,192.2 $[M - H]^-$ corresponding to desertomycin A. (*B*) Matrix-assisted laser desorption/ionization imaging mass spectrometry (MALDI-IMS) for desertomycin A. The microorganisms were grown directly on the object slide. The top picture of the mono- and the coculture represents a schematic overview of the position of the bacterial colony on TAP agar (monoculture) or on a split agar containing *C. reinhardtii* only in the right agar half (coculture). The bottom pictures show the overlays of the MALDI-IMS image indicating the color-coded abundance of ion *m/z* 1,214.9 ± 0.5 Da (desertomycin A, $[M + Na]^+$) and the actual culture. (*C*) *C. reinhardtii* treated with 1.5 μg · mL^{-1} desertomycin A forms gloeocapsoids. (Scale bars: 20 μm.) (*D*) Extracted ion chromatogram of an extract of a coculture of *C. reinhardtii* with *S. mashuensis* compared to a monoculture of the streptomycete. Extracted ion chromatogram of *m/z* 1,363.5 to 1,364.5 $[M - H]^-$ corresponding to monazomycin. (*E*) MALDI-IMS analysis. (*Top*) *S. mashuensis* colony on axenic TAP agar. (*Bottom*) *S. mashuensis* on TAP agar containing *C. reinhardtii*. MALDI-IMS images indicate color-coded abundance of ion *m/z* 1,387.3 ± 0.5 Da (monazomycin, $[M + Na]^+$). Color code: blue, low abundance and red, high abundance of ion. Mass spectrometry (MS) spectra of liquid chromatography–MS analyses were compared to an authentical standard for identification. (*F*) *C. reinhardtii* treated with 2.5 μg · mL^{-1} monazomycin with gloeocapsoid formation. (Scale bars: 20 μm.)

structural scaffold triggered phenotypically different aggregates or canonical palmelloids.

Gloeocapsoids Protect *C. reinhardtii* against Alkaline pH and Azalomycin F. Aggregate structures are often associated with protection (14). As gloeocapsoids are readily formed at neutral and alkaline pH under treatment with azalomycin F, we investigated their capacity to protect encapsulated cells. For this purpose, gloeocapsoid formation was induced by sublethal concentrations of azalomycin F at neutral pH. Then, gloeocapsoids and untreated control cells were inoculated in media with pH values between 9 and 11. After an initial drop, the autofluorescence of gloeocapsoid-derived cells readily recovered at pH 10 and 11, while that of the untreated cells showed no recovery (Fig. 4*A*). After 7 d of incubation at pH 10 and 11, the autofluorescence of gloeocapsoid-derived cells showed a significantly higher autofluorescence than the control cells (Fig. 4*B*). This was further demonstrated by plating

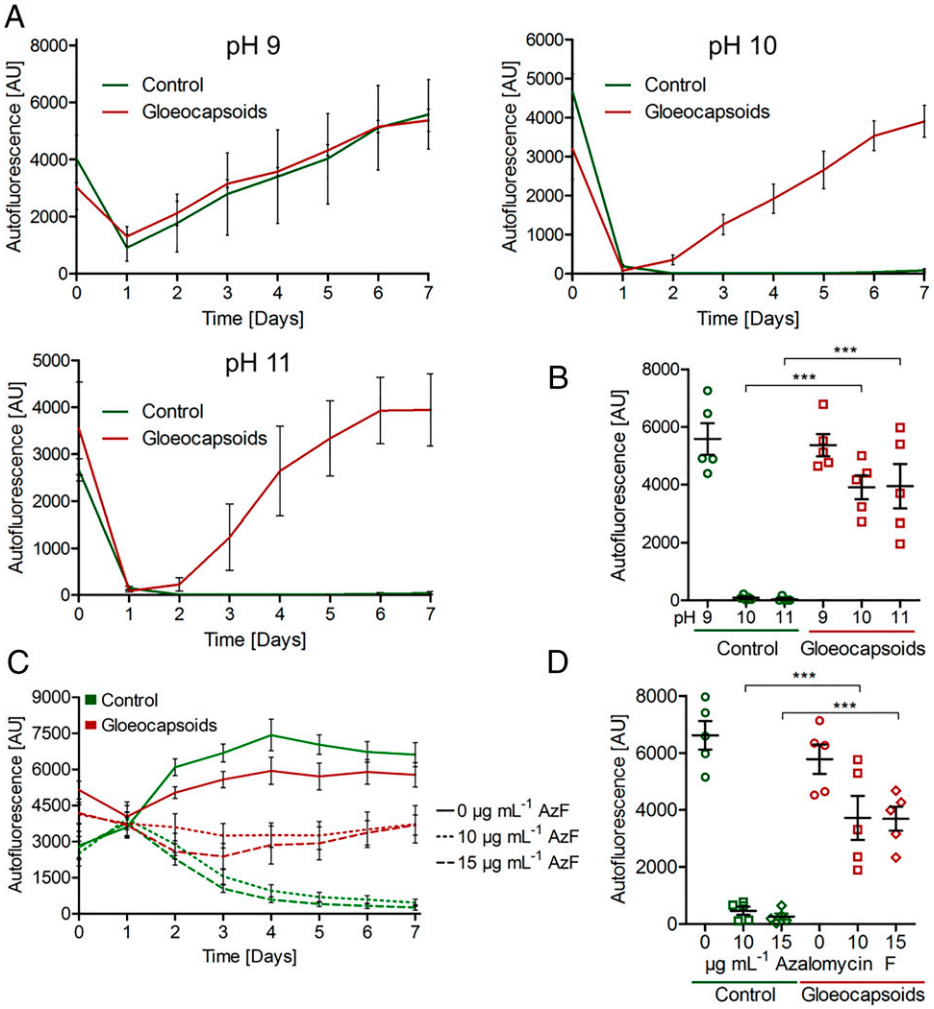

Fig. 4. Gloeocapsoid structures confer resistance to internalized cells against external stressors. (*A*) Control cells and gloeocapsoids of *C. reinhardtii* were inoculated into TAP media covering the pH range from 9 to 11. At pH 9, both vegetative cells and gloeocapsoid-derived cells grew. At pH 10 and pH 11, gloeocapsoid-derived cells regenerated after an initial drop in autofluorescence, whereas control cells showed no recovery. (*B*) Autofluorescence at day 7 of *C. reinhardtii* control cells and gloeocapsoids incubated in TAP medium from pH 7 to 9. (*C*) *C. reinhardtii* vegetative cells as well as gloeocapsoids were treated with 10 and 15 µg · mL^{-1} azalomycin F, and autofluorescence was monitored for 7 d. (*D*) Final autofluorescence at day 7 of *C. reinhardtii* control cells and gloeocapsoids treated with 0, 10, and 15 µg · mL^{-1} azalomycin F. For each time point, $n \geq 4$; SEMs are shown. ***$P \leq 0.001$ calculated using one-way ANOVA.

the cells on TAP agar after 7 d of incubation at pH 9 to 11 (*SI Appendix*, Fig. 10*A*), in which the cells derived from gloeocapsoids incubated at pH 10 and 11 formed colonies, an effect not observed for vegetative cells incubated at the same pH.

Next, the resistance of gloeocapsoids against lethal azalomycin F concentrations was tested. While the autofluorescence of untreated cells decreased steadily under the treatment with the toxin, the autofluorescence of gloeocapsoids remained stable (Fig. 4*C*). After 7 d of incubation, azalomycin F–treated gloeocapsoids showed a significantly higher autofluorescence compared to their azalomycin F–treated vegetative counterparts (Fig. 4*D*). Additionally, after 7 d of incubation, the cells were plated on TAP agar plates. Gloeocapsoids treated with 10 and 15 µg · mL^{-1} azalomycin F formed lawns of *C. reinhardtii* colonies, while vegetative cells treated with the same amounts of toxin only formed very few colonies (*SI Appendix*, Fig. 10*B*). By contrast, palmelloids induced by the addition of 100 mM NaCl and 15 mM sodium citrate to the medium did not protect *C. reinhardtii* against lethal concentrations of azalomycin F (*SI Appendix*, Figs. 11–14). Taken together, our data indicate that in contrast to canonical palmelloids, gloeocapsoids protect *C. reinhardtii* against alkaline pH and against azalomycin F at otherwise lethal concentrations.

Discussion

Multicellular Gloeocapsoids Represent a Defense Strategy against Both Alkaline pH and Azalomycin F. Microorganisms face ever-changing conditions in their respective habitats. Because of acids or bases released by microorganisms or farming, the environmental pH values can vary considerably between 3 and 10 (27, 41). By the uptake of acetate, *C. reinhardtii* increased the pH around its colonies. Under these conditions, the natural product azalomycin F produced by *S. iranensis* displayed reduced algicidal activity (*SI Appendix*, Fig. 2). This explains why a higher azalomycin F concentration was needed to induce gloeocapsoids in *C. reinhardtii* at pH 8 than at pH 7. It is remarkable that gloeocapsoids protect *C. reinhardtii* both against alkaline pH and azalomycin F since streptomycetes can increase their surrounding pH by the secretion of ammonia (27). Thus, an increase in pH in combination with algicidal marginolactones are indicators for the presence of competing streptomycetes. As a response, *C. reinhardtii* forms gloeocapsoids that represent a protective response to the presence of these harmful bacteria (Fig. 5).

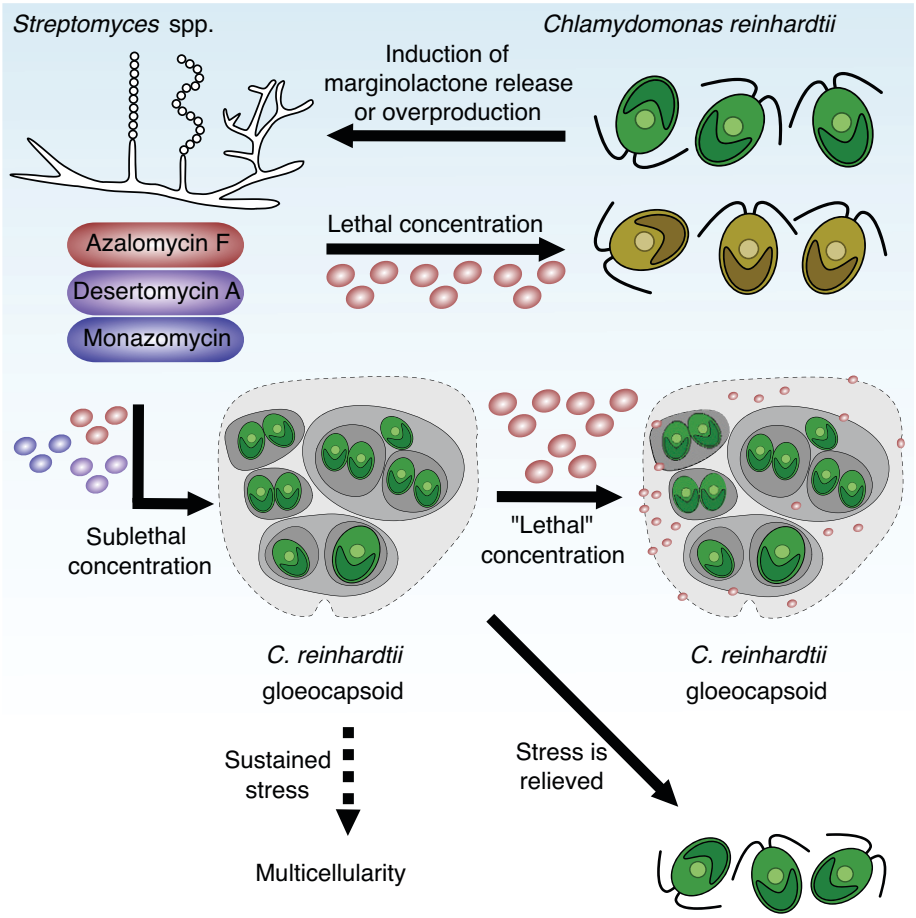

Fig. 5. Schematic overview of the interaction of *Streptomyces* spp. with *C. reinhardtii*. *C. reinhardtii* induces the release of the marginolactone azalomycin F as well as the overproduction and release of desertomycin A and monazomycin in cocultures with the bacteria *Streptomyces iranensis*, *Streptomyces macronensis*, and *Streptomyces mashuensis*. Lethal concentrations of these marginolactones lead to bleaching and death of *C. reinhardtii*. Sublethal concentrations trigger the formation of multicellular gloeocapsoids in which the individual cells are surrounded by multiple cell walls, membranes, and a spacious polysaccharide matrix. These aggregates protect the individual cells against otherwise lethal azalomycin F concentrations as well as alkaline pH, indicating the presence of competing streptomycetes. We hypothesize that the additional membranes and the acidic polysaccharide matrix sequester the positively charged azalomycin F, and hence, the algicide cannot reach the individual algal cells. After stress is relieved, the gloeocapsoids disassemble and motile single cells emerge. We hypothesize that sustained sublethal stress leads to the evolution of a multicellular organism exhibiting differentiated cell types and division of labor.

We have shown that *C. reinhardtii* required up to 7 d to develop gloeocapsoids, and therefore concentrations of 10 and 15 $\mu g \cdot mL^{-1}$ of azalomycin F killed non-pretreated algal cells within 24 h (Fig. 5) (24). *C. reinhardtii* only formed resistant gloeocapsoids at sublethal azalomycin F concentrations. This reflects an ecological scenario in which *C. reinhardtii* is not instantly confronted with high concentrations of an algicide but rather with a concentration gradient. It is worth noting that this might be a reason for the unusual release mechanism of azalomycin F. *S. iranensis* steadily produces the compound but only secretes it in the presence of *C. reinhardtii* (24). Production, storage, and massive release of the algicide upon contact with *C. reinhardtii* might be a strategy of the bacteria to circumvent the algal resistance mechanism by instantly creating a high concentration of azalomycin F.

Multicellularity Is a Widespread Protective Mechanism against Environmental Stressors. We provide evidence that aggregation facilitates the protection of single cells against environmental stressors. This is in accordance with observations made for, e.g., *Pseudomonas aeruginosa*, that produces biofilms in contact with antibiotics (42) or when experiencing DNA replication stress (43). A number of stressors induce the formation of palmelloids and actively formed aggregates in *C. reinhardtii* (14). Most likely, they play a role in protecting *C. reinhardtii* against these stressors. Since the main difference of NaCl- and sodium citrate–induced palmelloids and azalomycin F–induced gloeocapsoids is their protection against azalomycin F (Fig. 4 and *SI Appendix*, Figs. 11–14), we assigned gloeocapsoids to the family of palmelloids as specialized structures for defense against azalomycin F.

The matrix of gloeocapsoids is composed of acidic polysaccharides, which may have the capacity to buffer alkaline pH and might help to maintain an internal pH near 7. Similarly, sulfate-reducing bacteria buffer the surrounding pH by secretion of exopolysaccharides (44). The acidic polysaccharide matrix could also explain the resistance of gloeocapsoids against azalomycin F (Fig. 4 *C* and *D* and *SI Appendix*, Fig. 10*B*). We hypothesize that the guanidyl moiety of azalomycin F is positively charged at physiological pH and thus may be sequestered by the negatively charged acidic polysaccharides of the extracellular matrix. Furthermore, membranes are known targets of azalomycin F (24). Since there are several membrane layers present in gloeocapsoids (*SI Appendix*, Fig. 4*A*), this might promote sequestration of azalomycin F over a larger surface area (Fig. 2*B*). Possibly, the additional surrounding membranes sequester

marginolactones and thus protect the cytoplasmic membranes of cells lying underneath (Fig. 5). A similar protective mechanism appears to be realized in the tripartite system examined recently. The mycelium of *A. nidulans* is proposed to provide an increased surface area composed of polar lipids that function to sequester free azalomycin F, thereby protecting the cohabitating *C. reinhardtii* (24).

The formation of multicellular gloeocapsoids represents a protective strategy that does not require any other microbial partner organism. From an evolutionary point of view, such a strategy is in accordance with the theory that multicellularity initially evolved for survival in a hostile environment (45). Multicellularity is the fundamental step in the evolution of all higher organisms such as animals (46, 47) and enables maintenance of internal homeostasis even in the presence of osmotic stress, extreme pH, toxins, or desiccation (45, 48). This is also evident in the multicellular volvocine algae of the order *Chlamydomonadales*, *Pleodorina* and *Volvox* (49). These algae produce extracellular matrices, which enable the differentiation of soma and germ cells and also protect offspring developing inside the parent spheroid (49). Here, we report that *C. reinhardtii* produces a similar type of polysaccharide matrix. We highlight that the ability to form polysaccharide matrices is already present in the most basal member of the volvocine algae and might have been fundamental for the evolution of true multicellularity. This is also reflected in the low number of species-specific genes in *Volvox carteri* compared to *C. reinhardtii* (50). However, an essential difference found between *Volvox* and *C. reinhardtii* gloeocapsoids is the missing cytoplasmic connection between the individual cells, which enables *Volvox* cells to synchronize their behavior (51). Additionally, the polysaccharide matrix found in gloeocapsoids is linked to specific bacterial triggers and thus is formed for protection against harmful bacteria and could have later resulted in an evolution of multicellularity as suggested by similar experiments from Khona et al. (6). We hypothesize that multicellular green algae might have evolved by the sustained presence of bacterial marginolactones granting protection against these widespread algicides.

Algicidal Marginolactones Are Widespread in Nature. The marginolactones azalomycin F, desertomycin A, and monazomycin exhibit similar structures and target the cell membrane (37, 38, 52, 53). Sublethal doses of these natural products induce the formation of gloeocapsoids in *C. reinhardtii*. By contrast, amphotericin B and daptomycin, which also target the membrane by binding to ergosterol (39) or interfering with membrane microdomains (54), respectively, did not induce formation of gloeocapsoids (*SI Appendix*, Figs. 7–9). Thus, it is not merely membrane stress that leads to gloeocapsoids but rather the specific activity of marginolactones. For desertomycin A, it was shown that its activity depends on the primary amine on the side chain (55). This is supported by the observation that inactive members of the desertomycin family, the oasomycins, lack a primary amine in their side chain. The substitution of this side chain with side chains containing a primary or secondary amine created oasomycin derivatives with antibacterial activity (55). Our data further support the notion that the activity of marginolactones relies on their positively charged side chain.

Since marginolactones have been isolated from a number of actinobacteria, it can be expected that these compounds are widespread in soil habitats (56, 57). Bioinformatic analyses show that the azalomycin F biosynthetic gene cluster is present in a number of streptomycetes isolated from diverse soil samples across the world (58–61). We previously showed that azalomycin F was specifically released by *S. iranensis* in the presence of *C. reinhardtii* and possesses algicidal activity against several algal species (24). Similarly, we demonstrated here that *S. macronensis* and *S. mashuensis* overproduced their respective marginolactones in the presence of *C. reinhardtii* (Fig. 3). It is tempting to speculate that the streptomycetes create a spatially confined lethal concentration of marginolactones in soil to kill neighboring algae. It is worth noting that desertomycin G was isolated from a marine streptomycete present on the surface of a macroalga (62).

Our data suggest that marginolactones may have evolved to target algae. The widespread distribution of marginolactone-producing bacteria makes it likely that the compounds affect *C. reinhardtii* in its natural habitat. The alga in turn developed a particular strategy for defense against these compounds that includes the aggregation of cells, production of a polysaccharide matrix, and maintenance of multiple cell membranes. This structure, which we named gloeocapsoid, allows *C. reinhardtii* to cope with marginolactones and alkaline pH stress.

Materials and Methods

Microbial Strains and Plasmids. Microbial strains used in this study are listed in *SI Appendix*, Table 1.

Production and Purification of Azalomycin F from *S. iranensis*. Azalomycin F was produced and purified as described in Krespach et al. (24).

Preparation of Solid TAP Medium with pH Indicator and for Evaluation of Killing of *C. reinhardtii* by *S. iranensis*. TAP agar was prepared as published by Gorman and Levine (63). As a pH indicator, 0.03 $g \cdot L^{-1}$ bromothymol blue (Sigma-Aldrich) was added prior to the autoclaving of the medium. For TAP agar without acetate, the pH of the agar was adjusted to 6 by the addition of HCl. *C. reinhardtii* was spot inoculated and incubated at 26 °C and 30 $\mu E \cdot m^{-2} \cdot s^{-1}$.

For the evaluation of the killing of the algae by *S. iranensis*, *C. reinhardtii* was centrifuged with 2,000 × *g* for 2 min and inoculated into agar that was allowed to cool to ~35 °C. The final optical density at a wavelength of 750 nm (OD_{750}) was adjusted to 2. *S. iranensis* was washed with TAP medium (centrifugation 12,000 × *g* for 1 min), and 15 μL was spot inoculated onto agar containing *C. reinhardtii*. The coculture was incubated at 26 °C and 30 $\mu E \cdot m^{-2} \cdot s^{-1}$ and after 7 d, pictures were taken of the agar plates.

Staining Methods. The staining of *C. reinhardtii* with concanavalin A, Alcian blue, SYTOX blue, CellMask, and Nile red are explained in *SI Appendix*, *Staining methods*.

Induction of Formation of Gloeocapsoids for Resistance Assays. For the standardized induction of the formation of gloeocapsoids, 200 μL *C. reinhardtii* cell suspension (OD_{750} = 1) was precultured in TAP medium pH 7 for 7 d at 26 °C and 120 rpm at 30 $\mu E \cdot m^{-2} \cdot s^{-1}$ with 3 $\mu g \cdot mL^{-1}$ azalomycin F in 96-well plates. Control cells were not treated with the compound. After 7 d, cells from the same treatment were pooled and centrifuged at 2,000 × *g* for 2 min. The pellet was resuspended in fresh TAP medium to create a suspension with a final autofluorescence of 3,000. For the evaluation of resistance against pH, the pH of the fresh TAP medium was set to a final pH of 9 to 11 using NaOH. The test was carried out by the inoculation of 200 μL cell suspension into each well of a 96-well plate.

For testing resistance against azalomycin F, the cell pellet was resuspended in TAP medium of pH 7 to achieve a final autofluorescence of 3,000 (9×10^5 – 1×10^6 cells mL^{-1}), and 200 μL culture was inoculated into each well of a 96-well plate. Either 10 or 15 $\mu g \cdot mL^{-1}$ azalomycin F were added to each well when indicated. Incubation was carried out at 26 °C, 120 rpm, and 30 $\mu E \cdot m^{-2} \cdot s^{-1}$. Each 96-well plate was incubated at 26 °C, 120 rpm, and 30 $\mu E \cdot m^{-2} \cdot s^{-1}$. Autofluorescence, a proxy for the viability of *C. reinhardtii* (28), was measured after excitation at 480 nm, and emission was recorded at 684 nm on a Tecan Infinite M200 pro microplate reader (Tecan Trading AG).

Electron Microscopy. Sample preparation and electron microscopy are described in *SI Appendix*, *Electron microscopy*.

Data Availability. All study data are included in the article and/or *SI Appendix*.

ACKNOWLEDGMENTS. We thank Maria Mittag and Daniel Scheer for sharing their valuable expertise in the biology of *C. reinhardtii*. Volker Schroeckh is thanked for his continuous support and helpful critical discussions. Christina Täumer is acknowledged for excellent technical support. We are grateful to Hendrik Huthoff for the critical reading of the manuscript. This work was

funded by the Deutsche Forschungsgemeinschaft (German Research Foundation)—Project-ID 239748522—Sonderforschungsbereich (SFB) 1127, A02, B01, B02, and the Cluster of Excellence Balance of the Microverse—Project-ID 390713860, Gepris 2051.

1. T. Netzker *et al.*, Microbial interactions trigger the production of antibiotics. *Curr. Opin. Microbiol.* **45**, 117–123 (2018).
2. S. Sasso, H. Stibor, M. Mittag, A. R. Grossman, From molecular manipulation of domesticated *Chlamydomonas reinhardtii* to survival in nature. *eLife* **7**, e39233 (2018).
3. S. M. Shimmel, W. M. Darley, Productivity and density of soil algae in an agricultural system. *Ecology* **66**, 1439–1447 (1985).
4. S. S. Merchant *et al.*, The *Chlamydomonas* genome reveals the evolution of key animal and plant functions. *Science* **318**, 245–250 (2007).
5. J. de Vrieze, The littlest farmhands. *Science* **349**, 680–683 (2015).
6. D. M. Khona *et al.*, Characterization of salt stress-induced palmelloids in the green alga, *Chlamydomonas reinhardtii*. *Algal Res.* **16**, 434–448 (2016).
7. K. Iwasa, S. Murakami, Palmelloid formation of *Chlamydomonas* I. Palmelloid induction by organic acids. *Physiol. Plant.* **21**, 1224–1233 (1968).
8. K. Iwasa, S. Murakami, Palmelloid formation of *Chlamydomonas* II. Mechanism of palmelloid formation by organic acids. *Physiol. Plant.* **22**, 43–50 (1969).
9. K. Nakamura, D. F. Bray, E. B. Wagenaar, Ultrastructure of *Chlamydomonas eugametos* palmelloids induced by chloroplatinic acid treatment. *J. Bacteriol.* **121**, 338–343 (1975).
10. Y. Olsen, G. Knutsen, T. Lien, Characteristics of phosphorus limitation in *Chlamydomonas reinhardtii* (Chlorophycaceae) and its palmelloids. *J. Phycol.* **19**, 313–319 (1983).
11. I. Visviki, D. Santikul, The pH tolerance of *Chlamydomonas applanata* (Volvocales, Chlorophyta). *Arch. Environ. Contam. Toxicol.* **38**, 147–151 (2000).
12. G. Cheloni, V. I. Slaveykova, Morphological plasticity in *Chlamydomonas reinhardtii* and acclimation to micropollutant stress. *Aquat. Toxicol.* **231**, 105711 (2021).
13. A. Bajguz, L. Dinan, Effects of ecdysteroids on *Chlorella vulgaris*. *Physiol. Plant.* **121**, 349–357 (2004).
14. F. de Carpentier, S. D. Lemaire, A. Danon, When unity is strength: The strategies used by *Chlamydomonas* to survive environmental stresses. *Cells* **8**, 1307 (2019).
15. S. Sathe, P. M. Durand, Cellular aggregation in *Chlamydomonas* (Chlorophyceae) is chimaeric and depends on traits like cell size and motility. *Eur. J. Phycol.* **51**, 129–138 (2016).
16. J. Fan, L. Zheng, Y. Bai, S. Saroussi, A. R. Grossman, Flocculation of *Chlamydomonas reinhardtii* with different phenotypic traits by metal cations and high pH. *Front. Plant Sci.* **8**, 1997 (2017).
17. M. Lurling, W. Beekman, Palmelloids formation in *Chlamydomonas reinhardtii*: Defence against rotifer predators? *Ann. Limnol.* **42**, 65–72 (2006).
18. M. D. Herron *et al.*, De novo origins of multicellularity in response to predation. *Sci. Rep.* **9**, 2328 (2019).
19. A. A. Brakhage, Regulation of fungal secondary metabolism. *Nat. Rev. Microbiol.* **11**, 21–32 (2013).
20. P. Aiyar *et al.*, Antagonistic bacteria disrupt calcium homeostasis and immobilize algal cells. *Nat. Commun.* **8**, 1756 (2017).
21. V. Schroeckh *et al.*, Intimate bacterial-fungal interaction triggers biosynthesis of archetypal polyketides in *Aspergillus nidulans*. *Proc. Natl. Acad. Sci. U.S.A.* **106**, 14558–14563 (2009).
22. M. C. Stroe *et al.*, Targeted induction of a silent fungal gene cluster encoding the bacteria-specific germination inhibitor fumigermin. *eLife* **9**, e52541 (2020).
23. J. Fischer *et al.*, Chromatin mapping identifies BasR, a key regulator of bacteria-triggered production of fungal secondary metabolites. *eLife* **7**, e40969 (2018).
24. M. K. C. Krespach *et al.*, Lichen-like association of *Chlamydomonas reinhardtii* and *Aspergillus nidulans* protects algal cells from bacteria. *ISME J.* **14**, 2794–2805 (2020).
25. G. Cox, D. Benson, D. M. Dwarte, Ultrastructure of a cave-wall cyanophyte-*Gloeocapsa* NS4. *Arch. Microbiol.* **130**, 165–174 (1981).
26. Y. Shiraiwa, A. Goyal, N. E. Tolbert, Alkalization of the medium by unicellular green algae during uptake dissolved inorganic carbon. *Plant Cell Physiol.* **34**, 649–657 (1993).
27. M. Avalos, P. Garbeva, J. M. Raaijmakers, G. P. van Wezel, Production of ammonia as a low-cost and long-distance antibiotic strategy by *Streptomyces* species. *ISME J.* **14**, 569–583 (2020).
28. I. Pouneva, Evaluation of algal culture viability and physiological state by fluorescent microscopic methods. *Bulg. J. Plant Physiol.* **13**, 67–76 (1997).
29. W. Van Boekel, *Phaeocystis* colony mucus components and the importance of calcium ions for colony stability. *Mar. Ecol. Prog. Ser.* **87**, 301–305 (1992).
30. A. Pollio *et al.*, *Chlamydomonas pitschmannii* Ettl, a little known species from thermoacidic environments. *Protist* **156**, 287–302 (2005).
31. E. H. Harris, "Cell division" in *The Chlamydomonas Sourcebook: A Comprehensive Guide to Biology and Laboratory Use*, E. H. Harris, D. B. Stern, G. B. Witman, Eds. (Elsevier Science, 2009), **vol. 1**, pp. 65–87.
32. E. H. Harris, "Basal bodies, flagellar roots, and cellular filaments" in *The Chlamydomonas Sourcebook: A Comprehensive Guide to Biology and Laboratory Use*, E. H. Harris, D. B. Stern, G. B. Witman, Eds. (Elsevier Science, 2009), **vol. 1**, pp. 44–48.
33. G. Raposo, P. D. Stahl, Extracellular vesicles: A new communication paradigm? *Nat. Rev. Mol. Cell Biol.* **20**, 509–510 (2019).
34. Q. Cai, B. He, A. Weiberg, A. H. Buck, H. Jin, Small RNAs and extracellular vesicles: New mechanisms of cross-species communication and innovative tools for disease control. *PLoS Pathog.* **15**, e1008090 (2019).
35. M. Zerlin, R. Thiericke, Common principles in macrolactone (marginolactone) biosynthesis. Studies on the desertomycin family. *J. Org. Chem.* **59**, 6986–6993 (1994).
36. S. Benallaoua, J. Coulon, R. Bonaly, Membrane phospholipid composition in *Saccharomyces uvarum* cells grown in the presence of subinhibitory doses of amphotericin B and desertomycin. *Res. Microbiol.* **143**, 695–702 (1992).
37. O. S. Andersen, R. U. Muller, Monazomycin-induced single channels. I. Characterization of the elementary conductance events. *J. Gen. Physiol.* **80**, 403–426 (1982).
38. L. Becucci, R. Guidelli, Kinetics of channel formation in bilayer lipid membranes (BLMs) and tethered BLMs: Monazomycin and melittin. *Langmuir* **23**, 5601–5608 (2007).
39. T. M. Anderson *et al.*, Amphotericin forms an extramembranous and fungicidal sterol sponge. *Nat. Chem. Biol.* **10**, 400–406 (2014).
40. A. Müller *et al.*, Daptomycin inhibits cell envelope synthesis by interfering with fluid membrane microdomains. *Proc. Natl. Acad. Sci. U.S.A.* **113**, E7077–E7086 (2016).
41. E. W. Slessarev *et al.*, Water balance creates a threshold in soil pH at the global scale. *Nature* **540**, 567–569 (2016).
42. J. F. Linares, I. Gustafsson, F. Baquero, J. L. Martinez, Antibiotics as intermicrobial signaling agents instead of weapons. *Proc. Natl. Acad. Sci. U.S.A.* **103**, 19484–19489 (2006).
43. H. Gotoh *et al.*, *Pseudomonas aeruginosa*, under DNA replication inhibition, tends to form biofilms via Arr. *Res. Microbiol.* **159**, 294–302 (2008).
44. O. Braissant *et al.*, Exopolymeric substances of sulfate-reducing bacteria: Interactions with calcium at alkaline pH and implication for formation of carbonate minerals. *Geobiology* **5**, 401–411 (2007).
45. J. T. Bonner, The origins of multicellularity. *Integr. Biol. Issues News Rev.* **1**, 27–36 (1998).
46. T. Brunet, N. King, The origin of animal multicellularity and cell differentiation. *Dev. Cell* **43**, 124–140 (2017).
47. A. Woznica *et al.*, Bacterial lipids activate, synergize, and inhibit a developmental switch in choanoflagellates. *Proc. Natl. Acad. Sci. U.S.A.* **113**, 7894–7899 (2016).
48. N. A. Lyons, R. Kolter, On the evolution of bacterial multicellularity. *Curr. Opin. Microbiol.* **24**, 21–28 (2015).
49. A. Hallmann, Evolution of reproductive development in the volvocine algae. *Sex. Plant Reprod.* **24**, 97–112 (2011).
50. S. E. Prochnik *et al.*, Genomic analysis of organismal complexity in the multicellular green alga *Volvox carteri*. *Science* **329**, 223–226 (2010).
51. H. J. Hoops, I. Nishii, D. L. Kirk, "Cytoplasmic bridges in Volvox and its relatives" in *Cell-Cell Channels*, F. Baluska, D. Volkmann, P. W. Barlow, Eds. (Springer, 2006), pp. 65–84.
52. A. Bax, A. Aszalos, Z. Dinya, K. Sudo, Structure elucidation of the antibiotic desertomycin through the use of new two-dimensional NMR techniques. *J. Am. Chem. Soc.* **108**, 8056–8063 (1986).
53. B. S. Moore, C. Hertweck, Biosynthesis and attachment of novel bacterial polyketide synthase starter units. *Nat. Prod. Rep.* **19**, 70–99 (2002).
54. S. D. Taylor, M. Palmer, The action mechanism of daptomycin. *Bioorg. Med. Chem.* **24**, 6253–6268 (2016).
55. G. Kretzschmar, M. Krause, L. Radics, Chemistry and biological activity of oasomycin macrolactones. *Tetrahedron* **53**, 971–986 (1997).
56. X. Song, G. Yuan, P. Li, S. Cao, Guanidine-containing polyhydroxyl macrolides: Chemistry, biology, and structure-activity relationship. *Molecules* **24**, 3913 (2019).
57. R. G. S. Berlinck, A. F. Bertonha, M. Takaki, J. P. G. Rodriguez, The chemistry and biology of guanidine natural products. *Nat. Prod. Rep.* **34**, 1264–1301 (2017).
58. K. Blin *et al.*, antiSMASH 5.0: Updates to the secondary metabolite genome mining pipeline. *Nucleic Acids Res.* **47**, W81–W87 (2019).
59. J. Hamedi *et al.*, *Streptomyces iranensis* sp. nov., isolated from soil. *Int. J. Syst. Evol. Microbiol.* **60**, 1504–1509 (2010).
60. F. Horn *et al.*, Draft genome sequence of *Streptomyces iranensis*. *Genome Announc.* **2**, e00616-14 (2014).
61. K. H. Kim *et al.*, Natalamycin A, an ansamycin from a termite-associated *Streptomyces* sp. *Chem. Sci. (Camb.)* **5**, 4333–4338 (2014).
62. A. F. Braña *et al.*, Desertomycin G, a new antibiotic with activity against *Mycobacterium tuberculosis* and human breast tumor cell lines produced by *Streptomyces althioticus* MSM3, isolated from the Cantabrian Sea Intertidal macroalgae *Ulva* sp. *Mar. Drugs* **17**, 114 (2019).
63. D. S. Gorman, R. P. Levine, Cytochrome f and plastocyanin: Their sequence in the photosynthetic electron transport chain of *Chlamydomonas reinhardi*. *Proc. Natl. Acad. Sci. U.S.A.* **54**, 1665–1669 (1965).